

See discussions, stats, and author profiles for this publication at: <https://www.researchgate.net/publication/231664649>

# C–H···O Bonded Dimers in Liquid 4-Methoxybenzaldehyde: A Study by NMR, Vibrational Spectroscopy, and ab Initio Calculations

ARTICLE in THE JOURNAL OF PHYSICAL CHEMISTRY A · OCTOBER 1999

Impact Factor: 2.69 · DOI: 10.1021/jp990908f

---

CITATIONS

59

---

READS

30

3 AUTHORS, INCLUDING:



António M Amorim Da Costa

University of Coimbra

60 PUBLICATIONS 647 CITATIONS

SEE PROFILE



Paulo Ribeiro Claro

University of Aveiro

143 PUBLICATIONS 2,121 CITATIONS

SEE PROFILE

# C–H···O Bonded Dimers in Liquid 4-Methoxybenzaldehyde: A Study by NMR, Vibrational Spectroscopy, and ab Initio Calculations

N. Karger, A. M. Amorim da Costa, and Paulo J. A. Ribeiro-Claro\*

Unidade Química-Física Molecular, Departamento de Química, Faculdade de Ciências e Tecnologia, Universidade de Coimbra, P-3049 Coimbra, Portugal

Received: March 15, 1999; In Final Form: August 16, 1999

To further investigate the formation of C–H···O bonded dimers in liquid 4-methoxybenzaldehyde (4MeOB), previously suggested by Raman observations,  $^1\text{H}$  and  $^{17}\text{O}$  NMR chemical shift studies have been carried out for solutions of 4MeOB in  $\text{CCl}_4$ . In addition, Raman and FTIR spectra have been obtained and a set of ab initio calculations has been performed in order to determine possible dimer structures. Considering the  $^{17}\text{O}$  NMR spectra, the 15 ppm shielding effect observed for the carbonyl oxygen atom upon concentration increase is strong experimental evidence of hydrogen bonding in liquid 4MeOB. In addition to the previous Raman observations, this result clearly supports the engagement of the carbonyl group as an acceptor in a C–H···O hydrogen bond. The ab initio calculations at the HF/6-31G\* and B3LYP/6-31G\* levels suggest several possible dimer configurations whose relative energies are within a 5  $\text{kJ mol}^{-1}$  range. All the structures found present two hydrogen bond contacts, and the most stable ones have two carbonyl oxygen donors. The most significant dimer forms in the liquid phase are expected to arise from these configurations.

## Introduction

Weak hydrogen bonds of the form C–H···O have recently found increased interest.<sup>1–7</sup> While the bonding contribution of these hydrogen bonds rarely exceeds 8  $\text{kJ mol}^{-1}$ , much weaker than the conventional O–H···O bonds, it is now well established that C–H···O interactions play an important role in a wide variety of chemical and biochemical phenomena. The importance of these kinds of interactions in crystal packing and supramolecular design can be evaluated from recent reviews.<sup>1,2</sup> More exciting is the evidence that has accumulated in the past decade to show that C–H···O hydrogen bonds are key interactions in the structure and activity of biological systems.<sup>4–6</sup> The occurrence of C–H···O hydrogen bonds in the active sites of enzymes such as serine hydrolases<sup>6</sup> and their contribution to the helicoidal structure of RNA molecules instead of the often suggested O–H···O interactions<sup>5</sup> are two relevant examples. However, most of the experimental results reported refer to the crystalline state, and the information on the role of C–H···O interactions in the liquid phase is quite scarce.

In a previous work, Ribeiro-Claro et al.<sup>7</sup> suggested the existence of dimers in liquid 4-methoxybenzaldehyde (4MeOB, Figure 1) based on Raman observations. By performing dilution studies, they were able to show that the doublet found in the C=O stretching mode cannot be explained by Fermi resonance, as it was suggested earlier.<sup>8</sup> Also, the temperature dependence of the relative intensities of this doublet is more pronounced than in other bonds and indicates an interaction considerably stronger than the cis–trans equilibrium. A  $\Delta H$  value of  $-7.6 \pm 0.9 \text{ kJ mol}^{-1}$  corresponding to the formation of the dimers was derived from a Van't Hoff plot, while a dimerization energy of ca. 7  $\text{kJ mol}^{-1}$  was predicted from ab initio calculations.<sup>7</sup>

The 4MeOB molecule presents several potential donors and acceptors for weak hydrogen bonding. The most efficient hydrogen bond acceptor in the molecule is undoubtedly the carbonyl oxygen atom, but the presence of other acceptors such

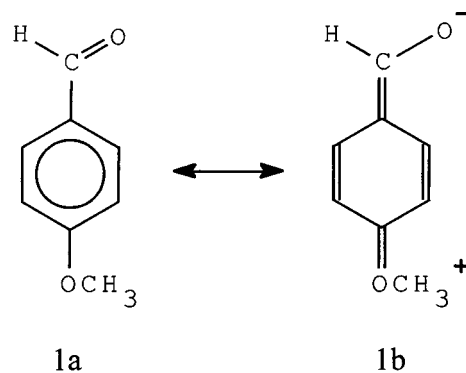


**Figure 1.** Chemical structure of 4MeOB molecule (a) showing the resonance structure with charge transfer from the methoxy group to the aldehyde group (b).

as the methoxy oxygen and the aromatic  $\pi$ -electron system cannot be ignored. The strongest C–H donor is not so easy to identify. The ability of the aldehyde proton to be a hydrogen bond donor has been a matter of controversy,<sup>9</sup> while the participation of methoxy and ring C–H bonds in C–H···O interactions has been observed for similar systems in the crystalline state (e.g., 2-methoxy-1,4-benzoquinone<sup>10</sup>). It should be noted that the  $\pi$ -electron transfer from the methoxy group to the aldehyde group (see resonance structure of Figure 1) will increase the ability of methyl protons and carbonyl oxygen to act as hydrogen bond donors and acceptor, respectively.

The purpose of the present study is to further investigate the existence and the structure of these C–H···O bonded dimers, using  $^1\text{H}$  and  $^{17}\text{O}$  NMR, Raman and FTIR vibrational spectroscopy, and ab initio calculations.

## Experimental and Calculations Section

4-Methoxybenzaldehyde and  $\text{CCl}_4$  were of analytical grade and obtained from Aldrich (Madrid, Spain).  $^1\text{H}$  NMR spectra showed no impurities and the liquids were used as supplied.

All the NMR spectra were run on a Varian Unity 500 NMR spectrometer (67.8 MHz for  $^{17}\text{O}$ ) at 298 K. For the proton spectra, a 5 mm probe was used and the spectra were referenced to a dilute solution of 3-(trimethylsilyl)propionate sodium salt in  $\text{D}_2\text{O}$  in a small capillary in the center of the sample tube. Four transients were accumulated, with a relaxation delay of 30 s. Chemical shifts are considered accurate to  $\pm 0.002$  ppm.

The natural abundance  $^{17}\text{O}$  spectra were obtained in a 10 mm broadband probe, with  $\text{D}_2\text{O}$  as the external reference and lock. A standard Cyclops pulse sequence was used, with a  $32\ \mu\text{s}$  ( $=90^\circ$ ) pulse width, 60 ms acquisition time, and 300 ms recycle delay. The number of transients accumulated ranged from 3000 to 45 000, depending on the concentration (from pure liquid to 0.02 mol fraction). Spectra were processed with a line broadening of 100 Hz to obtain reliable chemical shift values; the chemical shifts obtained are considered to be accurate to  $\pm 1$  ppm and  $\pm 3$  ppm for carbonyl and methoxy oxygen atoms, respectively. The observed line widths for  $^{17}\text{O}$  resonance lines are on the order of 1 kHz, but could not be evaluated quantitatively due to the low signal intensities. Nevertheless, an increase of line widths with rising 4MeOB concentration, probably due to the increase of bulk viscosity, was observed.

Raman spectra were recorded at room temperature on a triple monochromator (Jobin Yvon T 64000) using a CCD (Jobin Yvon Spectraview 2D) detector. The liquid samples were sealed in Kimax glass capillaries (i.d. 0.8 mm). The sample was illuminated by the 514.5 nm line of an  $\text{Ar}^+$  laser (Coherent-Inova 90) with 50 mW at the sample position. Entry and exit slits of the spectrometer were set to  $200\ \mu\text{m}$ , while the slit between premonochromator and spectrograph was opened to 14 mm, giving a resolution of approximately  $3\ \text{cm}^{-1}$ . The error in wavenumber is estimated to be smaller than  $1\ \text{cm}^{-1}$ .

Infrared spectra of liquid samples at room temperature were recorded in the  $400\text{--}4000\ \text{cm}^{-1}$  region with a Nicolet model 740 spectrometer, using a globar source, a DTGS detector and potassium bromide cells. The spectra were collected in 32 scans with a resolution of ca.  $2\ \text{cm}^{-1}$ . The errors in wavenumbers are estimated to be less than  $1\ \text{cm}^{-1}$ .

Ab initio calculations were performed using the Gaussian 98 program package<sup>11</sup> running on a personal computer. Molecular structures were fully optimized at the Hartree–Fock 6-31G\* and B3LYP/6-31G\* standard levels,<sup>11</sup> starting from several distinct dimer geometries. Harmonic vibrational wavenumbers were calculated at the HF level using analytic second derivatives to confirm the convergence to minima on the potential surface and to evaluate the zero-point vibrational energies (ZPVE). The calculated wavenumbers were always scaled by the standard factor of 0.9. The basis set superimposition error (BSSE) correction for the dimerization energies has been estimated by counterpoise calculations using the MESSAGE option of Gaussian 98.

## Results and Discussion

**$^1\text{H}$  and  $^{17}\text{O}$  NMR Spectra.** Figure 2 shows the concentration dependence of the proton chemical shifts for 4MeOB/ $\text{CCl}_4$  solutions. Since the protons bound directly to the ring carbon atoms show the same concentration dependence, only their average was included in the figure.

The concentration dependence of  $^1\text{H}$  chemical shifts is on the order of tenths of ppm, well below the 5–10 ppm shifts reported for conventional  $\text{O—H}\cdots\text{O}$  hydrogen bonds, but within the range of the observed values for  $\text{C—H}\cdots\pi$  interactions.<sup>12</sup> If the protons bound directly to the ring carbon atoms are assumed to reflect the change in the bulk susceptibility, then the protons

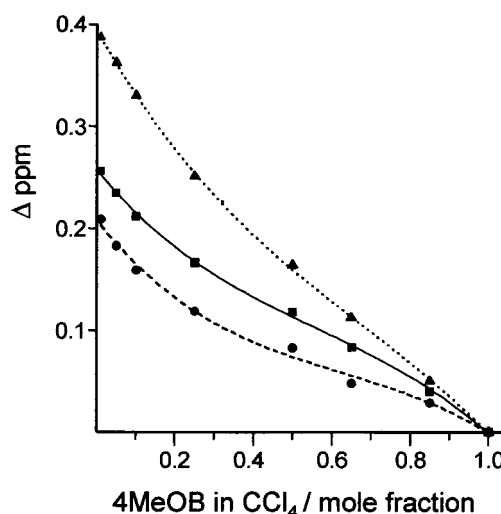


**Figure 2.** Concentration dependence of the proton chemical shifts of 4MeOB in  $\text{CCl}_4$  solutions, relative to the pure liquid: (■) average of ring protons; (●) aldehydic proton; (▲) methoxy protons.

of the methoxy group become slightly shielded upon increasing the 4MeOB concentration, while the proton of the aldehyde group becomes deshielded. This could indicate hydrogen bonding of the aldehyde proton. On the other hand, if the change in bulk susceptibility is better described by the methoxy protons, then both aldehyde and ring protons could be engaged in hydrogen bonding. However, one should note that these fairly small changes are in the same order of magnitude of the benzene ring anisotropy effect<sup>13</sup> and this effect can be felt differently by different protons in the molecule. Hence, no definite conclusion regarding hydrogen bonding should be drawn from these proton chemical shifts.

A different situation arises in the case of the  $^{17}\text{O}$  chemical shifts. Several studies<sup>14–19</sup> have concentrated on the  $^{17}\text{O}$  chemical shifts of substituted benzaldehyde and anisole derivatives. It was found that the carbonyl- $^{17}\text{O}$  chemical shift ( $\delta_{\text{carbonyl}}$ ) moves to lower frequency upon hydrogen bonding, either intramolecular with OH groups or intermolecular with alcoholic solvents.<sup>14–17</sup> The effect is on the order of 10–18 ppm shielding for intermolecular hydrogen bonds.<sup>14,15</sup> The influence of hydrogen bonding on the methoxy- $^{17}\text{O}$  chemical shift ( $\delta_{\text{methoxy}}$ ) is not so clear. It was found<sup>19</sup> that electron-withdrawing groups in the para position decrease shielding of the methoxy oxygen atom in anisole derivatives.

Figure 3 shows the  $^{17}\text{O}$  chemical shifts of 4MeOB in  $\text{CCl}_4$  as a function of the mole fraction of 4MeOB, ranging from  $x = 0.02$  to  $x = 1.0$ . The  $\delta_{\text{carbonyl}}$  and  $\delta_{\text{methoxy}}$  values compare with previously reported values for a 4MeOB/ $\text{CCl}_4$  solution.<sup>20</sup> The broad NMR signals obtained for the methoxy oxygen atom, resulting in large error bars associated with the  $\delta_{\text{methoxy}}$  points, do not allow a clear evaluation of its concentration dependence. The apparent presence of two distinct effects dominating the high and low concentration regions can result from the conjugation of bulk susceptibility effect and electron withdrawal by hydrogen bonding (either directly, with the methoxy group being an acceptor or a C—H donor, or indirectly, with polarization of the electron cloud by the hydrogen bonded carbonyl group).

In what concerns the carbonyl oxygen atom, Figure 3 shows a smooth continuous drop of  $\delta_{\text{carbonyl}}$ , from 557 ppm at  $x = 0.02$  to 542 ppm in the pure liquid. This 15 ppm shielding effect observed for the carbonyl oxygen atom upon concentration increase is strong evidence of hydrogen bonding in liquid 4MeOB. In addition to the previous Raman observations, this

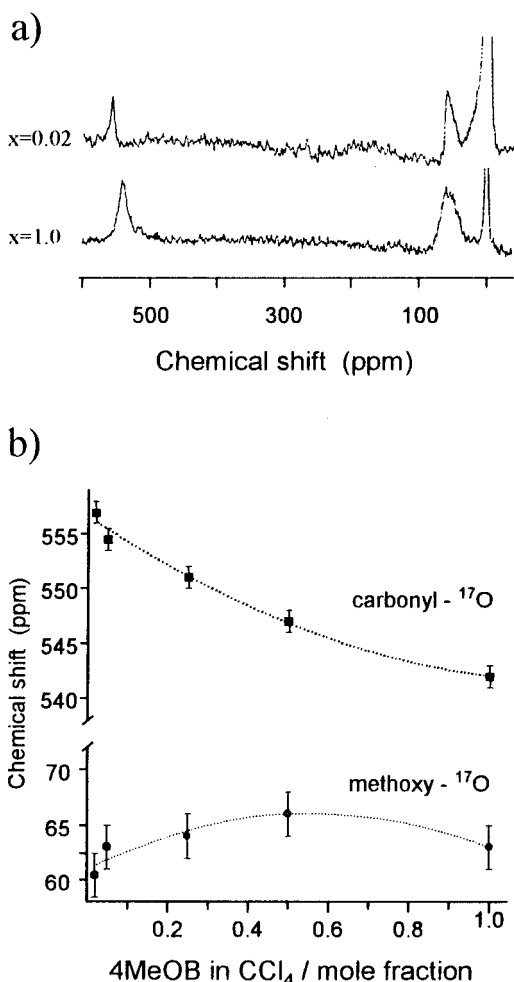


**Figure 3.** (a)  $^{17}\text{O}$  NMR spectra of 4MeOB, pure liquid and  $x = 0.02$  solution in  $\text{CCl}_4$ . (b) Concentration dependence of the  $^{17}\text{O}$  chemical shifts of 4MeOB in  $\text{CCl}_4$  solutions, referenced to external  $\text{D}_2\text{O}$ : (■) carbonyl oxygen nucleus; (●) methoxy oxygen nucleus. The line across the methoxy oxygen shifts is just an eye guide.

result clearly supports the engagement of the carbonyl group as an acceptor in a  $\text{C}-\text{H}\cdots\text{O}$  hydrogen bond.

**Ab initio Calculations.** Figure 4 shows the optimized geometry for the most significant dimer configurations found at the HF/6-31G\* and B3LYP/6-31G\* levels. Interestingly, there were no important dimers found in the configurational space containing only one  $\text{C}-\text{H}\cdots\text{O}$  interaction. The single hydrogen bonded species generally fell to one of the structures shown in Figure 4 during geometry optimization.

All the dimer structures shown present at least one carbonyl oxygen as a hydrogen bond acceptor. In structure **V**, the methoxy oxygen atom is also involved in a longer distance  $\text{C}-\text{H}\cdots\text{O}$  contact, and structure **III** has a  $\text{C}-\text{H}\cdots\pi$  interaction. Nevertheless, the most stable forms found in this calculation are those with two  $\text{C}-\text{H}\cdots\text{O}_{\text{carbonyl}}$  hydrogen bonds. In what concerns the  $\text{C}-\text{H}$  donors, both the aldehydic  $\text{C}-\text{H}$  and ring  $\text{C}-\text{H}_{\text{ortho}}$  bonds participate in the most stable dimer structures (**I** and **II**). The equivalent structures with ring  $\text{C}-\text{H}_{\text{meta}}$  donors have much lower stability (ca.  $7 \text{ kJ mol}^{-1}$  above). The methoxy  $\text{C}-\text{H}$  bonds give rise to longer distance interactions, as is the case for structure **VI**, with two methoxy  $\text{C}-\text{H}$  donors.

Table 1 collects the hydrogen bonding energies of the optimized dimers **I**–**VI**. The dimer structure **IV** is the lowest energy minimum for the  $(4\text{MeOB})_2$  system at the HF level, but several other structures can be found within  $5 \text{ kJ mol}^{-1}$ . Since

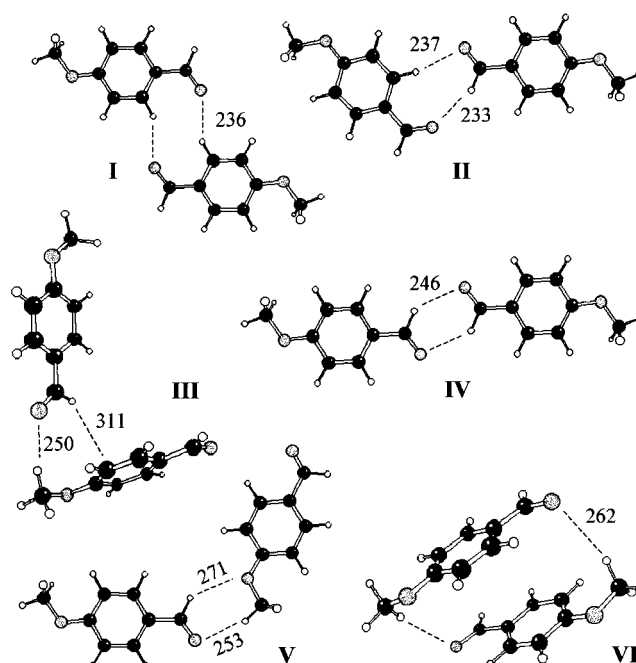


**Figure 4.** B3LYP/6-31G\* optimized geometries for the six lowest energy dimers of 4MeOB; hydrogen bond distances are given in pm; the calculated dimerization energies for each dimer are listed in Table 1; selected vibrational frequencies can be found in Table 2.

**TABLE 1: Dimerization Energies (Dimer –  $2 \times$  Monomer) and Relative Energy of Dimers of 4MeOB<sup>a</sup>**

	dimer					
	I	II	III	IV	V	VI
$\Delta E_{\text{dimerization}}/\text{kJ mol}^{-1}$						
6-31G*	-13.5	-15.4	-13.8	-16.0	-11.5	-9.7
after ZPVE	-11.7	-13.3	-12.2	-13.9	-9.8	-8.6
after CP	-9.5	-11.1	-9.2	-11.4	-7.6	-4.1
after CP+ZPVE	-7.7	9.0	-7.5	-9.3	-5.9	-3.0
B3LYP/6-31G*	-19.2	-19.0	-18.0	-16.2	-16.5	-13.7
$\Delta E_{\text{dimer}}/\text{kJ mol}^{-1}$						
6-31G*	2.5	0.6	2.2	0.0	4.5	6.2
after ZPVE	2.3	0.7	1.8	0.0	4.2	5.3
B3LYP/6-31G*	0.0	0.2	1.2	3.0	2.7	5.6

<sup>a</sup> Absolute energy of structure **I** =  $-914.637685 E_h$  at the HF/631G\* level and  $-920.204595 E_h$  at the B3LYP/6-31G\* level.

the value of  $RT$  at 300 K is ca.  $2.5 \text{ kJ mol}^{-1}$ , all these structures can contribute to the liquid-phase interactions. It should be noted that 4MeOB has two stable conformations (cis or trans orientation of carbonyl and methoxy groups relative to each other) separated by  $0.17 \text{ kJ mol}^{-1}$  at the HF/6-31G\* level.<sup>7</sup> In this way, all the trans + trans dimer structures shown in Figure 4 have the corresponding trans + cis and cis + cis combinations within a few tenths of  $\text{kJ mol}^{-1}$ . The uncorrected HF dimerization energies are in the range of  $12\text{--}16 \text{ kJ mol}^{-1}$ , somewhat larger than expected for a  $\text{C}-\text{H}\cdots\text{O}$  dimerization and well above the experimental value ( $7.6 \pm 0.9 \text{ kJ mol}^{-1}$ ).<sup>7</sup> Correction for BSSE or ZPVE reduces these values to the  $4\text{--}11$  and  $9\text{--}14 \text{ kJ mol}^{-1}$  ranges, respectively. Correction for both BSSE and ZPVE is expected to lead to overcorrected dimerization energies, because the ZPVE is not calculated for the BSSE corrected surface. It should be mentioned that a procedure to evaluate the BSSE changes in the potential energy surface in hydrogen bonded dimers has been proposed recently.<sup>21</sup> Changes are observed in both the calculated geometries and vibrational frequencies. The geometry optimization in the BSSE corrected surface leads to a larger hydrogen bond distance and a smaller



**TABLE 2: HF/6-31G\* Wavenumbers of the C=O and CH<sub>3</sub> Stretching Modes for the Monomer and Corresponding Wavenumber Shifts (Relative to the Monomer) for the Six Lower Energy Dimers of 4MeOB**

	monomer ( $\nu/\text{cm}^{-1}$ )	dimer ( $\Delta\nu/\text{cm}^{-1}$ )					
		I	II	III	IV	V	VI
$\nu\text{C=O}$	1796	-11 -7	-23 -8	-18 -3	-30 -14	-14 -1	-13 -11
$\nu\text{CH}$	2837	-2 -1	-1 74	-4 19	65 64	0 33	-5 -4
$\nu\text{CH}_3$ s	2893	-2 -2	-1 -1	2 10	0 0	1 1	5 5
$\nu\text{CH}_3$ as	2952	-3 -3	-2 -2	2 21	0 0	0 1	12 12
$\nu\text{CH}_3$ as	3002	-3 -3	-3 -2	2 2	-2 -2	0 29	2 2
$\nu\text{CH}$ ring	3021	-2 -2	-2 4	-3 2	5 5	0 2	-4 -3
$\nu\text{CH}$ ring	3052	9 9	-1 5	-2 1	3 3	-3 0	0 0
$\nu\text{CH}$ ring	3067	13 15	-1 5	-2 0	-7 -7	-2 0	-1 0
$\nu\text{CH}$ ring	3070	-2 -2	-1 -1	2 9	2 2	1 4	1 2

hydrogen bond stretching frequency (as expected), but not always to a decrease of the ZVPE.<sup>21</sup>

The inclusion of electron correlation effects is known to be important in the study of hydrogen bonding systems. Table 1 also presents the relative energies of the dimers and the dimerization energies at the B3LYP/6-31G\* level. Although the same structures can be found within the same 5 kJ mol<sup>-1</sup> interval, there are some changes in the relative energies of the dimers. The absolute minimum is now the structure **I**, with structure **IV** 3.0 kJ mol<sup>-1</sup> above.

An interesting issue is the evaluation of the maximum strength of a single C-H...O bond in this system. Because of the total electron interactions and the cooperative effects, such energy is expected to be less than half the interaction energy of the dimer forms with two equivalent hydrogen bonds (e.g., forms **I** and **IV**). Calculations on dimer structures with geometrical constraints to allow only one hydrogen bond contact yield single C-H...O interaction energies in the range of 3–5 and 5–7 kJ mol<sup>-1</sup> for HF/6-31G\* and B3LYP/6-31G\* levels, respectively. These values are in agreement with reported estimates of similar C-H...O interactions in acetone<sup>22</sup> and acetic acid.<sup>23</sup>

The calculated vibrational frequencies for the dimer structures can be used to predict the wavenumber shifts upon dimerization. This is particularly interesting in the case of the stretching modes of C=O and C-H bonds ( $\nu\text{C=O}$  and  $\nu\text{C-H}$ ), since these oscillators are directly involved in the bonding interactions and give rise to well localized (single oscillator) normal modes.

As it can be seen from Table 2, the different dimer structures lead to different dimerization shifts. The wavenumber of the  $\nu\text{C=O}$  mode drops by ca. 11–18 cm<sup>-1</sup> from monomer to dimers **III**, **V**, and **VI**. These values agree with the 16 cm<sup>-1</sup> shift observed in both Raman and FTIR spectra. The calculated shift for dimer **II** is somewhat larger (–23 cm<sup>-1</sup>) but it is still comparable with the experimental one. For dimers presenting *C*<sub>2h</sub> symmetry (**I** and **IV**) two  $\nu\text{C=O}$  bands are predicted, with opposite vibrational activities: the symmetric mode, Raman active, and the antisymmetric mode (IR active). However, the two predicted  $\nu\text{C=O}$  bands have close wavenumbers in dimer **I** and only for dimer **IV** they are clearly distinct.

The CH stretching modes display an interesting behavior, the ab initio results predict a decrease in the C–H bond length when

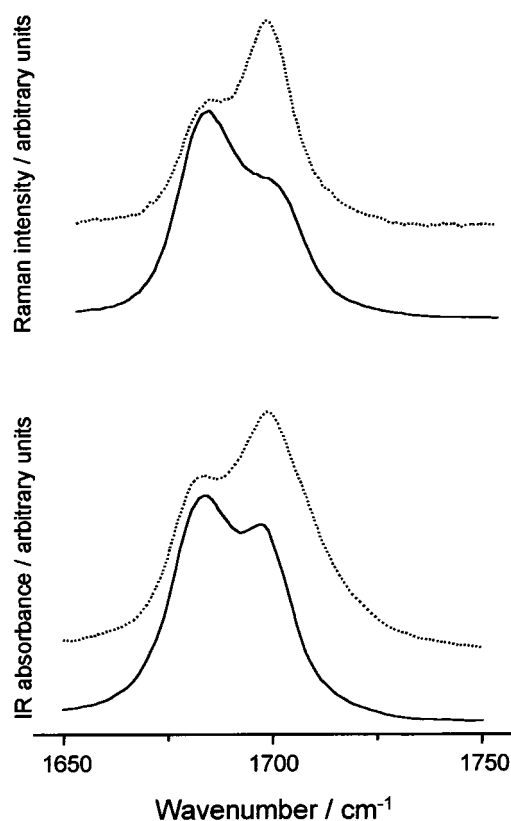


**Figure 5.** Room-temperature Raman and FTIR spectra of pure 4MeOB (solid line) and diluted 4MeOB, *x* = 0.1 in CCl<sub>4</sub> (dashed line), in the region of the C=O stretching modes.

the C–H is involved in hydrogen bonding, leading to an increase of the pertinent  $\nu\text{CH}$  mode up to 70 cm<sup>-1</sup> (see Table 2). This unexpected result, decrease of bond length due to hydrogen bonding, has been obtained previously for CH...O bonding in different molecular systems presenting weak C–H donors<sup>23–25</sup> (with single or multiple hydrogen bonds) and has found some experimental support from <sup>13</sup>C NMR<sup>25</sup> and vibrational<sup>26</sup> data. The expression of this phenomenon in the vibrational spectra has not been fully understood<sup>26</sup> and deserves further investigation.

**Vibrational Spectra.** The occurrence of dimeric forms of 4MeOB in the liquid phase was first suggested<sup>7</sup> by the observation of two  $\nu\text{C=O}$  bands in the vibrational spectra (see Figure 5), one of which is believed to represent the hydrogen bonded group, as discussed above.

The presence of a single  $\nu\text{C=O}$  band ascribed to the dimer in both the Raman and IR spectra provides some clues about the possible structure of the dimer. In particular, the absence of the two distinct bands predicted for dimer **IV** indicates that the pure *C*<sub>2h</sub> structure is not present in the liquid phase. On the other hand, structures such as **III** and **V** allow the formation of 4MeOB chains (trimers, tetramers, ...) that would give rise to new bands in the lower wavenumber side of the dimer band due to cooperative strengthening of hydrogen bonds. The absence of these bands suggests that such oligomers do not give significant contributions to the liquid structure.

Additional information can be obtained from the  $\nu\text{CH}$  modes. Figure 6 shows the Raman and FTIR spectra in the  $\nu\text{CH}$  region of pure and diluted 4MeOB. Upon dilution in CCl<sub>4</sub>, several changes occur in the  $\nu\text{CH}$  region of 4MeOB; the CH<sub>3</sub> stretch modes gain in intensity, while the line width of both CH<sub>3</sub> and ring CH modes decreases. The most prominent aldehydic  $\nu\text{CH}$

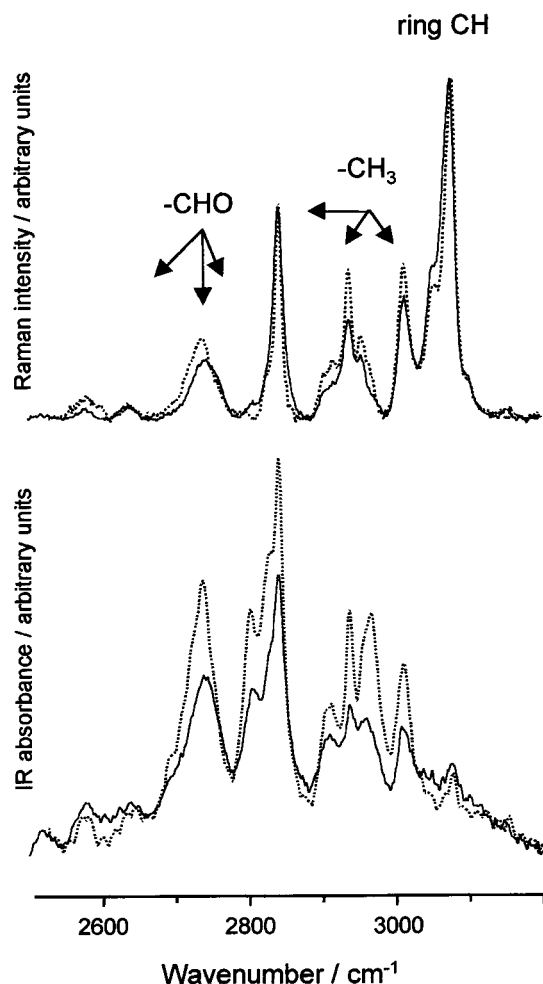


**Figure 6.** Room-temperature Raman and FTIR spectra of pure 4MeOB (solid line) and diluted 4MeOB,  $x = 0.1$  in  $\text{CCl}_4$  (dashed line), in the region of the C–H stretching modes.<sup>27</sup>

band increases in intensity and shifts to lower wavenumber (or loses intensity in the high wavenumber side).

These changes are not very strong and not easy to interpret, since at least the aldehydic mode is confounded by Fermi resonance with overtones of ring modes. Also, some of these changes could be due to a changing solvent environment. However, both the decrease of intensity and the increase of line width of the CH modes observed for the pure liquid relative to the solution are consistent with the presence of hydrogen bond interactions. In fact, this same behavior was recently observed in the  $\nu\text{C-H}$  modes of caffeine hydrate upon the formation of  $\text{C-H}\cdots\text{O}$  bonds.<sup>28</sup> The changes in the aldehydic  $\nu\text{CH}$  band can also be related to the presence of two kinds of CH bands (due to monomer and dimer forms), the latter disappearing upon dilution. Being so, a straightforward interpretation of these spectra stresses the importance of the aldehydic C–H bond as the donor in the  $\text{C-H}\cdots\text{O}$  interaction, without discarding the participation of both the methoxy and ring CH bonds.

## Conclusions

The  $^{17}\text{O}$  NMR investigations of 4MeOB/ $\text{CCl}_4$  mixtures provide strong support for the existence of  $\text{CH}\cdots\text{O}$  bonded dimers of 4MeOB in the liquid phase, as it was suggested previously on the grounds of Raman observations.<sup>7</sup> In fact, the  $^{17}\text{O}$  chemical shift of the carbonyl group rises by 15 ppm with increasing dilution in  $\text{CCl}_4$ , a value that parallels the observed

values for  $\text{O-H}\cdots\text{O}$  interactions in substituted benzaldehyde/alcohol mixtures.

In what concerns the structure of the dimers, all the experimental and computational results are consistent with the carbonyl oxygen atom being the hydrogen bond acceptor. Less clear indications were found, however, to assign unambiguously the C–H donor. Both the  $^1\text{H}$  NMR results and the  $\nu\text{C-H}$  vibrational spectra can be interpreted as favoring the aldehydic C–H bond as the dominant hydrogen bond donor in this molecule, but the possible participation of the methoxy and ring C–H donors cannot be discarded.

Ab initio calculations provide important additional information. At the HF/6-31G\* level, the most stable form has  $C_{2h}$  symmetry, with a double  $\text{C-H}\cdots\text{O}$  bond between both aldehydic groups. However, the  $\nu\text{C=O}$  band pattern predicted for a pure  $C_{2h}$  structure is not supported experimentally. When electron correlation effects are considered using the DFT approach (B3LYP/6-31G\* level), the lowest energy structures are those with ring  $\text{C-H}_{\text{ortho}}$  donors, but a distinction between ortho and meta protons is not observable in the  $^1\text{H}$  NMR. At both levels of calculation, the several dimer configurations have relative energy differences within a  $5 \text{ kJ mol}^{-1}$  range. One may expect that the most significant (with longest lifetime) dimer forms in the liquid phase arise from these configurations.

It should be noted that the energetic (enthalpic) factor is not the only one to be considered in this dimerization process, as the entropy change on the process is not independent of the dimer structure formed. In particular, due to the presence of the  $-\text{CHO}$  and  $-\text{O-CH}_3$  internal rotations in the monomer, the entropic part of the  $\text{C-H}\cdots\text{O}$  interaction must be in favor of those dimer structures that keep the maximum conformational freedom (only form **IV**) and penalize those with internal rotation restrictions (all the remaining forms, the extreme case being dimer **VI**, with all internal rotations restricted).

**Acknowledgment.** This work was supported by grants from the European Community HCM program (CHRX-CT94-0466) and from the Fundação para a Ciência e Tecnologia, FCT, Lisboa. We thank Prof. M. Pereira dos Santos of the Universidade de Minho, Braga, for the opportunity to record the Raman spectra in his laboratory and Mr. Rui Rodrigues for his help in obtaining the NMR spectra.

## References and Notes

- (1) Desiraju, G. R. *Acc. Chem. Res.* **1996**, 29, 441.
- (2) Steiner, Th. *Chem. Commun.* **1997**, 727.
- (3) Jedlovsky, P.; Turi, L. *J. Phys. Chem.* **1997**, 101, 5429.
- (4) Wahl, C. M.; Sundaralingam, M. *Trends Biochem. Sci.* **1997**, 22, 97.
- (5) Auffinger, P.; Westhof, E. *J. Mol. Biol.* **1997**, 274, 54.
- (6) Derewenda, Z. S.; Derewenda, U.; Kobos, P. M. *J. Mol. Biol.* **1994**, 241, 83.
- (7) Ribeiro-Claro, P. J. A.; Batista de Carvalho, L. A. E.; Amado, A. M. *J. Raman Spectrosc.* **1997**, 28, 867.
- (8) Nyquist, R. A. *Appl. Spectrosc.* **1992**, 46, 306.
- (9) Nishio, M.; Hirota, M.; Umezawa, Y. *The CH/ $\pi$  interaction: evidence, nature, and consequences*, 1st ed.; Wiley-VCH: New York, 1998; Chapter 4.
- (10) Keegstra, E. M. D.; Spek, A. L.; Zwikker, J. W.; Jenneskens, L. W. *J. Chem. Soc., Chem. Commun.* **1994**, 1633.
- (11) Frisch, M. J.; Trucks, G. W.; Schlegel, H. B.; Scuseria, G. E.; Robb, M. A.; Cheeseman, J. R.; Zakrzewski, V. G.; Montgomery, J. A.; Stratmann, R. E.; Burant, J. C.; Dapprich, S.; Millam, J. M.; Daniels, A. D.; Kudin, K. N.; Strain, M. C.; Farkas, O.; Tomasi, J.; Barone, V.; Cossi, M.; Cammi, R.; Mennucci, B.; Pomelli, C.; Adamo, C.; Clifford, S.; Ochterski, J.; Petersson, G. A.; Ayala, P. Y.; Cui, Q.; Morokuma, K.; Malick, D. K.; Rabuck, A. D.; Raghavachari, K.; Foresman, J. B.; Cioslowski, J.; Ortiz, J. V.; Stefanov, B. B.; Liu, G.; Liashenko, A.; Piskorz, P.; Komaromi, I.; Gomperts, R.; Martin, R. L.; Fox, D. J.; Keith, T.; Al-Laham, M. A.; Peng,

C. Y.; Nanayakkara, A.; Gonzalez, C.; Challacombe, M.; Gill, P. M. W.; Johnson, B. G.; Chen, W.; Wong, M. W.; Andres, J. L.; Head-Gordon, M.; Replogle, E. S.; Pople, J. A. *Gaussian 98*, revision A.3; Gaussian Inc.: Pittsburgh, PA, 1998.

- (12) Reeves, L. W.; Schneider, W. G. *Can. J. Chem.* **1957**, 35, 251.
- (13) Harris, R. K. *Nuclear Magnetic Resonance Spectroscopy, a physicochemical view*; Pitman Books: London, 1983; Chapter 8.
- (14) Boykin, D. W.; Chandrasekaran, S.; Baumstark, A. L. *Magn. Reson. Chem.* **1993**, 31, 489.
- (15) Amour, Th. E. St.; Burger, M. I.; Valentine, B.; Fiat, D. *J. Am. Chem. Soc.*, **1981**, 103, 1128.
- (16) Jaccard, G.; Lauterwein, J. *Helv. Chim. Acta* **1986**, 69, 1469.
- (17) Delseeth, C.; Nguyen, T.; Kintzinger, J. P. *Helv. Chim. Acta* **1980**, 51, 489.
- (18) Kolehmainen, E.; Knuutinen, J. *Magn. Reson. Chem.* **1991**, 29, 520.
- (19) Katoh, M.; Sugawara, T.; Kawada, Y.; Iwamura, H. *Bull. Chem. Soc. Jpn.* **1977**, 52, 3475.

- (20) Dahn, H.; Pechy, P.; Toan, V. V. *Magn. Reson. Chem.* **1997**, 35, 598.
- (21) Simon, S.; Duran, M.; Dannenberg, J. J. *J. Chem. Phys.* **1996**, 105, 11024.
- (22) Turi, L. *Chem. Phys. Lett.* **1997**, 275, 35.
- (23) Turi, L.; Dannenberg, J. J. *J. Phys. Chem.* **1993**, 97, 12197.
- (24) Gil, F. P. S. C.; Teixeira-Dias, J. J. C. *J. Mol. Struct. Theochem* **1996**, 363, 311.
- (25) Vizzioli, C.; de Azua, M. C. R.; Giribert, C. G.; Contreras, R. H.; Turi, L.; Dannenberg, J. J.; Rae, I. D.; Weigold, J. A.; Malagoli, M.; Zanasi, R.; Lazzaretti, P. *J. Phys. Chem.* **1994**, 98, 8858.
- (26) Adcock, J. L.; Zhang, H. *J. Org. Chem.* **1995**, 60, 1999.
- (27) Roedger, N. P. G. *A Guide to the Complete Interpretation of Infrared Spectra of Organic Structures*; Wiley & Sons: London, 1994 and references therein.
- (28) de Matas, M.; Edwards, H. G. M.; Lawson, E. E.; Shields, L.; York, P. *J. Mol. Struct.* **1998**, 440, 97.